Lipid-cholesterol interactions

Monte Carlo simulations and theory

H. L. Scott
Department of Physics, Oklahoma State University, Stillwater, Oklahoma 74078-0444 USA

ABSTRACT Results of Monte Carlo calculations of order parameter profiles of lipid chains interacting with cholesterol are presented. Cholesterol concentrations in the simulations are sufficiently large that it is possible to analyze profiles for chains which are near neighbors of two or more cholesterol molecules, chains which are neighbors to a single cholesterol, and chains which are not near any cholesterol molecules. The profiles show that cholesterol acts to significantly decrease the ability of neighboring chains to undergo *trans-gauche* isomeric rotations, although these chains are not all forced into all-*trans* conformations. The effect is significantly greater for chains which are neighbors to more than one cholesterol. The Monte Carlo results are next used as a guide to develop a theoretical model for lipid-cholesterol mixtures. The properties of this model and the phase diagram which it predicts are described. The phase diagram is then compared with experimentally determined phase diagrams. The model calculations and the computer simulations upon which they are based yield a molecular mechanism for several of the observed phases exhibited by lipid-cholesterol mixtures. The theoretical model predicts that at low temperatures the system should exhibit solid phase immiscibility.

1. INTRODUCTION

Given that cholesterol is found in almost all animal cell membranes in concentrations up to 50% by weight, the inescapable conclusion is that an important role is played by this molecule in membrane behavior. Yet, after intensive study over the past two decades, this role is not precisely known. What has emerged from the experimental effort is a complex picture of the manner in which cholesterol affects the physical properties of lipids in bilayers (1). The sharp main lipid phase transition becomes weakened with increasing cholesterol concentration (2, 3) and a broad, diffuse transition appears at higher temperature (3). Around 25 mol % the main lipid phase transition disappears, and around 50 mol % the broad transition disappears. Above the chain melting transition the lipid chain mobility and average lateral area decrease with increasing cholesterol concentration (4, 5). At temperatures below the phase transition the lipid chain mobility is increased by the presence of cholesterol (6).

In addition to the above equilibrium measurements, there have been several NMR studies of the dynamical aspects of lipid-cholesterol interactions (7, 8). These studies indicate that cholesterol strongly affects the slower, cooperative molecular motions of the lipids but has a smaller effect on the fast timescale motions.

Phase diagrams for lipid-cholesterol mixtures have been proposed by a number of workers using ESR (9, 10), fluorescence anisotropy (11), neutron scattering (12), and, most recently, Deuterium NMR (13). In general the phase diagrams proposed are not in full agreement with each other, and are perhaps affected by the experimental probes in some cases. The recent phase diagram proposed by Vist and Davis (based upon differential scanning calorimetry and DMR experiments) is likely the most reliable because no perturbative techniques other than perdeuteration are involved. From their experiments Vist and Davis have identified a new lipid-cholesterol phase, which they call the β phase. The β phase is a high-cholesterol content phase in which lipid chains are generally highly ordered, but in which there is rapid translational and axial rotational motion of the lipid molecules. At temperatures below the main lipid chain melting temperature and at cholesterol concentrations between ~5% and ~23% the gel phase coexists with the β phase. At temperatures above the main chain melting phase transition there is a region of coexistence between the fluid lipid phase and the β phase. Near the pure lipid phase transition, at low cholesterol content, there is a narrow region of coexistence between gel and fluid lipid phases.

Ipsen et al. (14) have developed a theoretical model for cholesterol in lipid bilayers which reproduces the experimental phase diagram obtained by Vist and Davis. This model consists of a lattice with sites occupied by either cholesterol or DPPC (DPPC occupies two sites). All molecular degrees of freedom are stored in Ising variables which denote "ordered" or "disordered" chains, and Potts variables which denote different types of

0006-3495/91/02/445/11 $2.00

ordered states. Although far more degrees of freedom are associated with acyl chain conformations these are all contained within the single Ising "disorder" state, while the crystalline degrees of freedom are treated explicitly in the Potts variables. Presumably the Potts variables represent orientation of the ordered lipid in some manner. In the mean field approximation the parameters of this model can be set to values such that the phase diagram of Vist and Davis is reproduced. This effort is a useful first theoretical study of a complex problem, but by using point particles (with only *Ising-like* degrees of freedom) in a mean field approximation the model masks the interplay between the microscopic intermolecular interactions and correlations and the observed phase properties. What is still missing is a theory which unambiguously associates the observed properties of lipid-cholesterol mixtures with specific, direct microscopic interactions. This is in part because accurate and unambiguous theories are difficult to formulate and analyze, and also because the precise nature of the lipid-cholesterol interactions is not well understood.

In this paper we report the results of detailed Monte Carlo studies of the interactions between lipid chains and cholesterol in bilayers. We then describe how these results may be incorporated into a theoretical model for lipid bilayer phase transitions, and we show the predicted phase diagram for DPPC-cholesterol mixtures. In the next section we describe the Monte Carlo calculations, and present the results. In Section III we describe the theoretical model and the phase diagram the model predicts. In Section IV we compare our model results with the experimental phase diagram of Vist and Davis, and with the theory of Ipsen et al.

II. MONTE CARLO STUDIES OF LIPID-CHOLESTEROL INTERACTIONS

A. The Monte Carlo method

The Monte Carlo method has been used to study interactions between lipid chains and cholesterol at several cholesterol concentrations. This effort is an extension of an earlier simulation (15) in which a system consisting of a single cholesterol molecule in a planar array of 99 lipid chains of varying length was analyzed using the Monte Carlo (MC) method. The full details of the simulation technique have been published elsewhere (15, 16). As in the earlier work (15) the objective of the simulations is to calculate MC average order parameter profiles for chains which are near neighbors to cholesterol, and to compare these profiles with those for chains which are not close to cholesterol ("bulk chains"). The profiles are defined by:

$$S_n = \tfrac{1}{2}\langle 3\cos^2\theta_n - 1\rangle, \qquad (1)$$

where θ_n is the angular deviation of bond n from its orientation relative to the bilayer normal when the chain is in the all-*trans* state. We have shown earlier that this procedure produces order parameter profiles for chains which agree with the measured profiles from Deuterium NMR experiments (17). Furthermore, the average number of *gauche* bonds per chain is, after equilibration, 3.5 ± 0.1 per chain for DPPC, close to the value of 3.8 estimated from thermodynamic considerations (18).

We have now extended the earlier calculations to models with higher cholesterol concentration. Specifically, we have run MC simulations of the following systems: (*a*) 3 cholesterol molecules and 97 lipid chains of length C-14, C-16, and C-18. (*b*) 7 cholesterol molecules and 93 lipid chains of length C-14 only. (*c*) 13 cholesterol molecules and 87 lipid chains of length C-14 only.

In all cases the previously described procedures were followed (15, 16). Simulations were run at fixed area per chain of 30 Å^2, at $T = 300$ K (sufficient for chain disordering for all chains at the fixed molecular areas used). Equilibration consisted of 40×10^3 configurations per chain, and averages were calculated over a further $30\text{–}40 \times 10^3$ configurations per chain. Errors were estimated from fluctuations in values of the bond order parameters calculated at intermediate steps during each run. All simulations were run on the Cray XMP/48 at the National Center for Supercomputing Applications (Champaign-Urbana, IL).

B. Monte Carlo results

Figs. 1, *a* and *b*, show schematic pictures of a top view of the simulation cell for the systems consisting of seven and thirteen cholesterol molecules, respectively. Because the order parameter profiles for C-14 chains calculated in simulations of 3 cholesterols plus 97 chains proved to be nearly identical to those calculated in simulations of 7 cholesterols plus 93 chains, only results from the latter runs will be described in detail. The key difference between the lowest two and the highest cholesterol concentrations studied is (as shown in Fig. 1), at the lower concentrations no lipid chain is a near neighbor to more than a single cholesterol. For the 13 cholesterol plus 87 chain simulations, there are 24 chains which are near neighbors of two or three cholesterol molecules. In all cases the cholesterols are not allowed to undergo translational motion although the conforma-

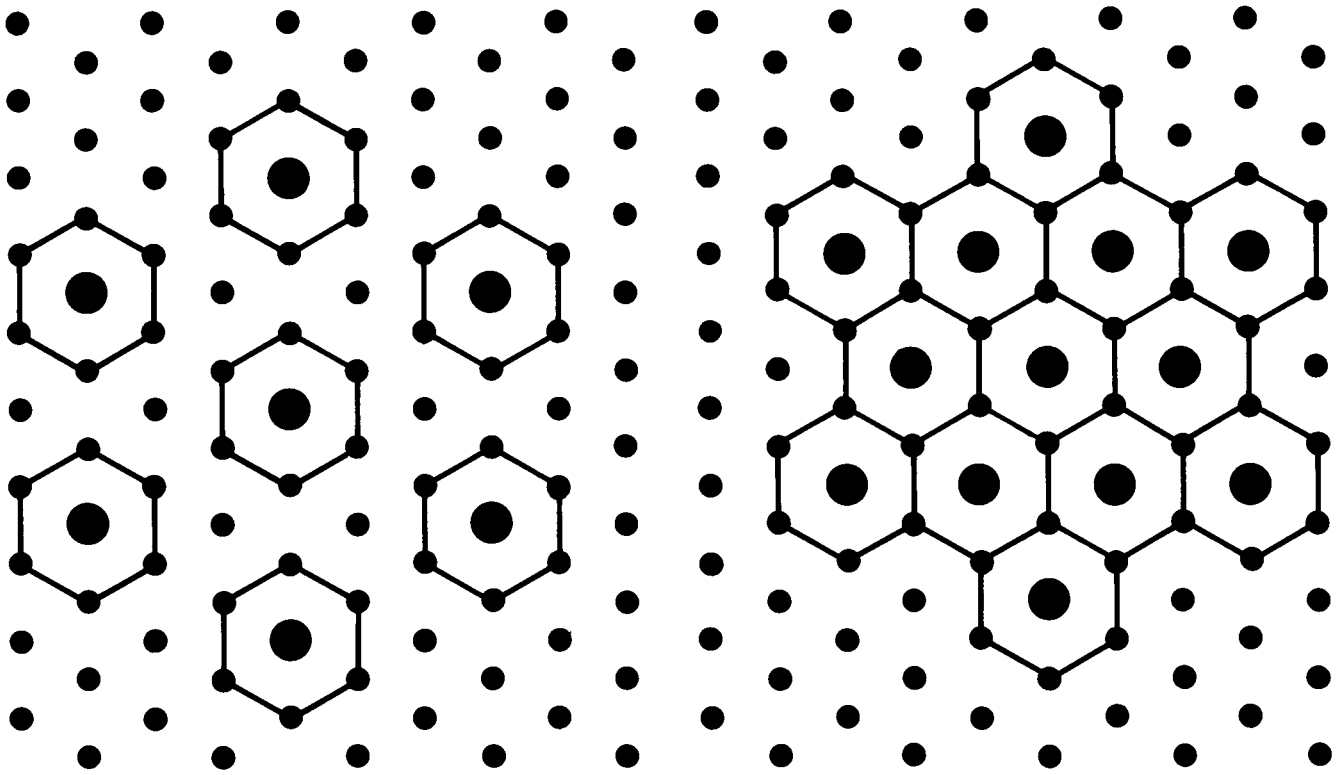

FIGURE 1 (*a*) Top view of a simulation array of 93 chains and 7 cholesterols. Small dots show locations of chains and large dots show locations of cholesterols. The near neighbors of the cholesterols are connected by lines. (b) Top view of a simulation array of 87 chains and 13 cholesterols. Small dots show locations of chains and large dots show locations of cholesterols. Neighbors of one or more cholesterols are connected by lines.

tions of the chains on each cholesterol are allowed to change.

Discussion of the results of the calculations will be confined in this paper to the simulations involving C-14 chains. The effect of increasing chain length has been described in reference 15 for chains which are neighbors to one cholesterol, and available computer time did not allow for extension of this aspect of the study to higher cholesterol concentrations.

Fig. 2 contains the major results from the simulations. This figure shows order parameter profiles calculated for chains which are near neighbor to more than one cholesterol (from the 87 chain–13 cholesterol simulations), chains which are near neighbor to a single cholesterol, and bulk chains (the latter two profiles from 93 chain–7 cholesterol simulations). In the 87 chain–13 cholesterol simulations there are fewer bulk chains (45) and chains which are neighbor to a single cholesterol (18) than in the 93 chain–7 cholesterol runs (58 and 42, respectively). This means that the profiles calculated in the latter simulations show smaller fluctuations due to finite size effects. Therefore the profiles calculated from

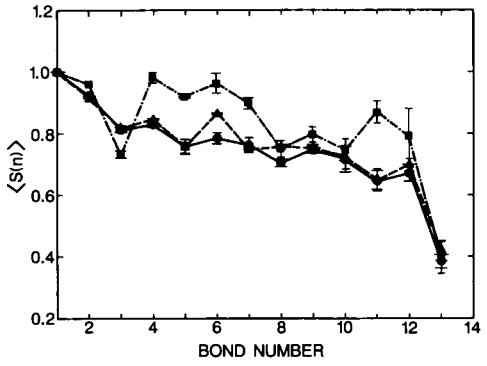

FIGURE 2 Plot of order parameter profiles, $\langle S(n) \rangle$, vs. bond number for bulk chains (*solid line*), chains neighbor to one cholesterol (*dashed line*), and chains neighbor to two or more cholesterols (*dot-dashed line*). Error bars are calculated as standard deviations in intermediate averages calculated during production runs as in reference 15.

the 93 chain–7 cholesterol simulations are more accurate for bulk chains and chains which are neighbors to one cholesterol only. Because the use of seven cholesterol molecules allows for better sampling of the lipid-cholesterol configuration space than the single cholesterol simulations did (15) (42 chains are near neighbors to a cholesterol instead of only 6), the profile for the chains which are neighbors to a single cholesterol molecule show fewer fluctuations due to small sample size than were found in reference 15. The profile for chains which are neighbors to a single cholesterol follows closely the profile for the bulk chains although the segments in the middle of the C-14 chains are slightly more ordered if the chain is a cholesterol neighbor, as in reference 15.

The profile in Fig. 2 for chains which are neighbors to more than one cholesterol molecule reveals that these chains are forced into configurations which are substantially more ordered than in the other profiles. The error bars on each of the profiles in Fig. 2 are indications of the extent to which the given bonds are able to change rotameric states after equilibrium is established. The smaller error bars for most bonds between 2 and 8 for the profile for chains adjacent to a single cholesterol are a consequence of the restrictions on the rotational mobility of these bonds. It is clear that, as in the earlier work, the cholesterol inhibits the rotameric freedom of its neighbor chains, although on average the neighbors are not in all-*trans* conformations. The profile for chains which are near neighbor to two or more cholesterols shows a sharp dip at bond #3 which reflects this inhibition. The dip has occurred because, on several of the chains included in this profile, a kink has formed which reorients bond #3 but leaves bonds 4–6 in *trans* orientations. The steric presence of the two cholesterol molecules makes this kink a relatively stable structure during the simulation. It is very difficult for a chain to undergo additional *gauche* rotations about its upper carbons in the steric presence of two cholesterols as well as other chains after equilibrium has been established.

Fig. 3 shows a typical configuration of a cholesterol and two neighbor chains, taken from part of a larger seven cholesterol C-14 simulation. This figure shows how the flat side of the cholesterol molecule is more likely to force a chain into an all-*trans* conformation, but the rougher side is not as likely to do this. The fact that error bars are larger for chains adjacent to two or more cholesterols may be a consequence of unusual free volume available to chains which are near two rough cholesterol faces, although simulation data is not sufficient for a definitive interpretation of this point.

The major conclusions to be drawn from the MC calculations are that (*a*) Cholesterol promotes ordering of chains which are initially in a fluid state, although the chains are not all forced into all-*trans* conformations. (*b*) This ordering is enhanced greatly for chains which are in near-neighbor contact with two or more cholesterol molecules. (*c*) Cholesterol reduces the freedom of neighbor chains to undergo *gauche* rotations. That is, the accessible configuration space of the chains is markedly diminished with increasing cholesterol content.

For the purpose of devising theoretical models based upon the simulations it would be helpful if the effects above could be expressed quantitatively in a simple mathematical function describing the decrease in chain states with increasing cholesterol content. Unfortunately the simulations only represent two data points in a plot of chain restrictions vs. cholesterol content. It is therefore impossible to uniquely quantify the nature of the restrictions imposed on the chains by the cholesterol. However, the *qualitative* trend is clear from Fig. 2, and it is possible to define a theoretical model on this basis. In the next section we describe such a model for lipid bilayers containing cholesterol.

III. THEORETICAL MODEL

A. Definition of the model

The MC calculations in the previous section provide insight into the interaction between lipid chains and cholesterol in bilayers. We now utilize this insight to define an analytical theoretical model for phase equilibria in lipid bilayers containing cholesterol. To this end, consider a flat monomolecular layer of DPPC molecules representing half of a full bilayer. Now consider a projection of the molecules in this layer onto a two-dimensional flat plane. Lipid molecules with all-*trans* bonds will roughly project as elongated rods with curved ends. Lipid molecules with *gauche* bonds will project as more complicated geometrical objects, but in a first approximation we may again imagine these to be rods with curved ends with different dimensions due to the displacement of the chains caused by the *gauche* bonds. We then have a two-dimensional fluid which consists of a collection of rods of different size and having different orientations in the plane. In this sense half of a lipid bilayer may be modeled as a purely two-dimensional fluid of hard rods with circular caps and with sizes determined by the rotameric states of the molecules. We show a schematic picture of the two-dimensional fluid and the various phases such a fluid may exhibit in Fig. 4.

The above mapping is not practical if each of the many rotameric states of a lipid molecule is assigned a uniquely shaped shadow. Therefore, as a refinement we suppose that all of the different rotameric states of the lipid

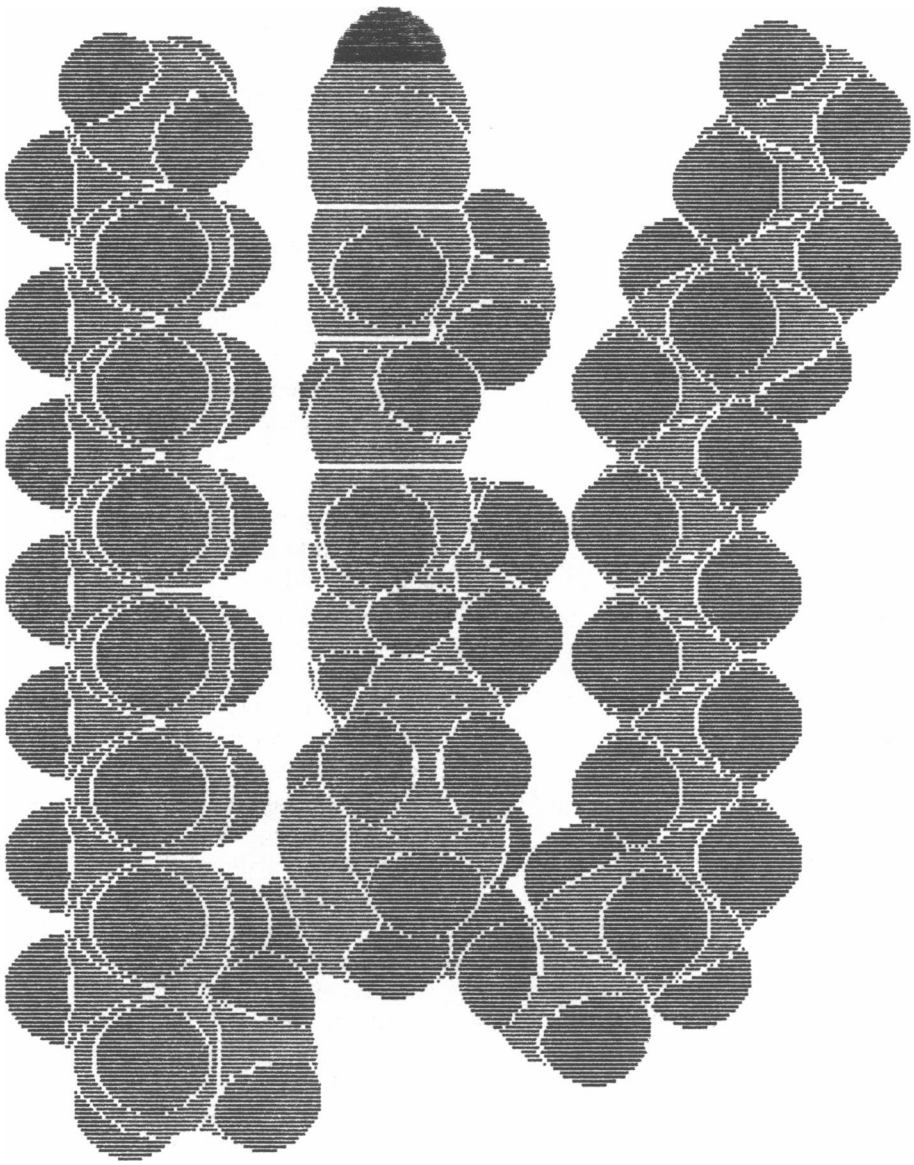

FIGURE 3 A typical configuration produced during the simulations showing two lipid chains adjacent to a single cholesterol. Note that it is easier for the chain adjacent to the flat side of the cholesterol to maintain an all-*trans* conformation.

chains may be grouped, as shadows, into a finite set of rods with circular caps, in which the rotameric states dictate the length of the rod. And, because more than one rotameric state may map onto similarly sized rods, a statistical weight is associated with each member of the set. The energetics of *trans-gauche* isomerization also require that an energy be assigned to each member of the class. To allow for different orientations of the shadows in the plane each shadow state is further assigned as many substates as there are allowed molecular orientations. In reality there should be a continuum of orientations, but this is clearly impractical. In this paper we follow reference 19 and explicitly consider only orientations which are multiples of 60°.

This approach was first utilized by the author as a basic model for the lipid bilayer chain melting transition using hard disks of varying radius for the shadows (20), and was later generalized to rod-shaped molecules with circular caps (19, 21). The advantage of this approach is that it is possible to calculate the thermodynamic properties of such a mixture of hard regularly shaped objects quite accurately using Scaled Particle Theory (22). We

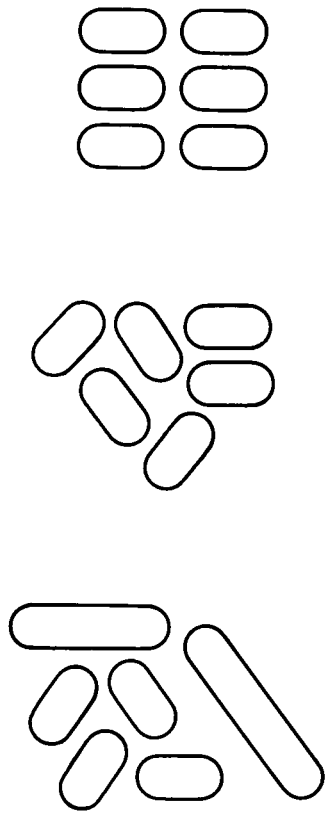

FIGURE 4 Schematic picture of the two-dimensional hard rod shadow fluid in three typical states. (*Top*) Orientational order and lipid chain order (only the smallest rod states are present). (*Middle*) Orientational isotropy and lipid chain order. (*Bottom*) Orientational isotropy and lipid chain disorder (all rod states are present).

let α_k denote the fraction of lipid molecules in shadow state k (which will denote a specific capped rod size and orientation), ω_k denote the statistical weight of this state, and ϵ_k denote the energy of the state due to the *gauche* rotations. Then the molar Free Energy at absolute temperature T may be written as:

$$\frac{G}{RT} = \sum_k \alpha_k \ln\left(\frac{\alpha_k}{\omega_k}\right) + \ln\left(\frac{\rho}{1 - \rho\Sigma_i \alpha_i A_i}\right) + \frac{1}{2}\left(\frac{\rho}{1 - \rho\Sigma_i \alpha_i A_i}\right)\sum_{k,l} \alpha_k \alpha_l \left(\pi \frac{d_k d_l}{2} + l_k d_l + d_l l_k + l_k l_l |\sin \theta_{k,l}|\right) + \sum_k \alpha_k \epsilon_k - \frac{C}{RT(A - 38)^{1.5}} + \frac{N_A \Pi A}{RT}. \quad (2)$$

Here R is the gas constant, ρ is the particle density, A_k is the projected area for a molecule in state k, and d_k and l_k denote the cap diameter and the rod length of the shadow associated with rod state k, respectively. $\theta_{k,l}$ is the orientation angle between rods in states k and l (restricted to multiples of 60°). C is an attractive energy constant and the expression involving C represents an integrated total attractive energy of the chains. II is the lateral pressure on the chains, fixed at the value of 50 dynes/cm as discussed in references 20 and 19, and A is the area per molecule (19). Table 1 gives the values of the dimensions of the rod states, the attractive interaction constants C for DPPC and cholesterol, the weights, and the average number of *gauche* states for each rod state. The energies ϵ_k are found by multiplying this latter value by 500 cal/mol. The hard rod cap sizes are the same as earlier (19) but the lengths are slightly changed. This is because in the earlier work the pretransition was identified partially by the onset of molecular long-axis rotation. Since it is now known that this transition is caused by different packing interactions (23–25) the shadow dimensions are readjusted so that at zero cholesterol concentration the lipid phase transition occurs at 41.4°C and involves *both* chain disordering and rotational disordering. The attractive interaction constant, C, is set equal to $1.26 \times 10^2 x_l + 1.20 \times 10^2 x_c$ kcal-Å^3/mol, where x_l is the lipid concentration, equal to

TABLE 1 Model properties (x_c is cholesterol concentration)

Lipid	Average no. of gauche rotations	Cap diameter	Length	Weight	Weight reduction factor
		Å	Å		
DPPC	0	5.25	3.58	1	1
	2	5.25	4.17	24	$1–4.5x_c$
	3.79	5.25	4.86	280	$1–4.5x_c$
	5.90	5.25	5.66	1328	$1–4.5x_c–3x_c^2$
	4.78	5.25	6.64	3288	$1–4.5x_c–3x_c^2$
	4.84	5.25	7.83	256	$1–4.5x_c$
	4.50	5.25	9.32	24	$1–4.5x_c$
CHOL	0	7.00	1.00	1	1

$1 - x_c$. This places the main lipid phase transition at zero cholesterol concentration in the model at 41.4°C.

The thermodynamic state of the system at a given temperature and lateral pressure II is found by minimizing G/RT with respect to the area per molecule A and the shadow state occupation variables α_k. In general there are many solutions of the minimization equations, and at any T and II one must search the solution space for the set of occupation variables which represents the absolute minimum of the Free energy. Phase transitions in a pure lipid system are identified by points at which the set of α_k which minimizes G/RT switches from, say, a set representing an ordered state (all α_k's zero except those representing the smallest size shadows), to a disordered state (in which the α_k's are all non-negligible). In this way the model was set up earlier to describe the main lipid bilayer phase transition. In addition, for a certain range of length-to-width ratios for the rods, two transitions occurred in the model. At a lower temperature the model changed from a state in which chains were ordered and the shadows were also orientationally ordered to a state in which the chains remained ordered but the orientational order vanished. Then at a higher temperature the system changed from a chain ordered to a chain melted state, as evidenced by the appearance of shadow states of all allowed sizes and orientations (19).

The model is extended to include cholesterol in the lipid system by picking the appropriate dimensions for the projection of the cholesterol molecule on the reference plane, and including states for the allowed orientations of the cholesterols. In Table 1 we list the values assigned to the cholesterol states. The cholesterol shadow cap diameter is larger than that for the lipids due to the protruding CH_3 groups, and the shadow length is smaller. The assigned hard core area of the cholesterol is, in this model, 45.4 Å^2, while the area of the smallest lipid shadow state is 40.4 Å^2. The area of the smallest *gauche* state shadow in the model is 43.5 Å^2, and the area of the next state is 47.2 Å^2. It must be remembered that these areas are "effective" molecular areas rather than actual areas of, say, CPK models (26). The reason for this is that hard objects pack at densities where the objects are in actual contact, while van der Waals forces in molecular systems prevent this. Therefore in the hard rod shadow fluid model for lipids, areas of the rods must be similar to the areas per molecule of the lipids and the cholesterol in the most dense gel phase.

To construct a realistic model for lipid-cholesterol bilayers it is also necessary to incorporate the cholesterol-lipid interactions observed in the simulations into the theoretical framework. In the model described above the natural way to include the restrictions on the rotameric freedom of the lipid chains which cholesterol induces is through the statistical weights associated with the hard rod states. In earlier work (19, 20) these weights were calculated from combinatorial arguments based on the number of isomeric states with given shadow dimensions. If the effect of cholesterol is to reduce the number of rotameric states available to the lipid molecules, then a straightforward way to include this in the model is to systematically reduce the weights as the cholesterol concentration increases. This is accomplished by multiplying each of the weights in Table 1 by a function which decreases with the cholesterol content x_c (but which is never negative). The MC results of the previous section suggest a linear x_c dependance for this function to account for the effect of isolated cholesterol molecules on neighboring lipids, and a quadratic x_c dependance due to stronger restrictions on lipid chains which are neighbors to two cholesterol molecules. The coefficients of the linear and quadratic terms should reflect both the number of chains affected by each isolated cholesterol or pair of cholesterols, and the degree to which the chains are restricted. However, the mapping of lipid chain states onto hard disks is not one-to-one, in that many more chain states are mapped into certain disk states. Because the manner in which a chain state is inhibited by steric interactions with cholesterol depends on the exact steric shape the chain takes, and because this level of detail is lost in the mapping onto two-dimensional rods, the MC calculated effects must be included in the model as *effective* interactions between the cholesterol shadow states and the rod shadow states. The coefficients used in this model for the linear and quadratic contributions to the reduction in statistical weights of the rod states are given in Table 1. This particular set is chosen mainly for simplicity and to obtain an initial phase separation line in the fluid phase at $x_c \sim 5\%$. The quadratic x_c dependence is inserted only for the states with the greatest weights, as these are most strongly affected by pairs of cholesterols. The linear weight reduction functions become zero at $x_c = 0.22$ and the quadratic functions vanish at $x_c = 0.20$ so that above 22 mol % cholesterol the fluid lipid shadow states are totally suppressed.

The extended model now contains a complex dependence on the cholesterol concentration, which can lead to phase separations. The procedure for calculating the lipid-cholesterol phase diagram for this model is as follows: (*a*) For fixed cholesterol concentration, temperature, and lateral pressure find the set of α_k's and area per molecule A for which the Free Energy, G in Eq. 1 is a true minimum. (*b*) Repeat the above step for each cholesterol concentration. (*c*) Plot the resulting Free Energy versus cholesterol concentration. (*d*) Thermody-

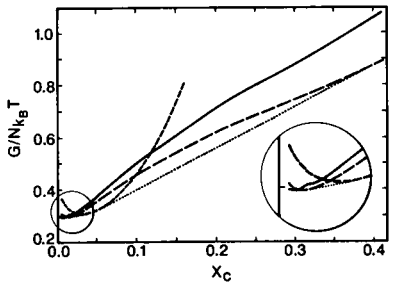

FIGURE 5 Typical plot of Gibbs Free Energy calculated after numerical solution of the minimization problem for T = 40°C. (*Small-dashed line*) fluid phase solution. (*Large dashed line*) Beta phase solution. (*Solid line*) $L_{\beta'}$ phase solution. The dotted lines are double tangent lines. The points at which these lines intersect the minimum free energy curve are the concentrations of the coexisting phases. The very low x_c region is enlarged, showing the emergence of the β phase as the dominant phase in this region.

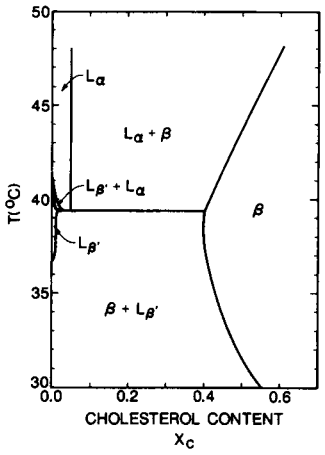

FIGURE 6 Phase diagram for the theoretical model. L_α denotes the fluid lipid phase and $L_{\beta'}$ denotes the ordered gel phase. β denotes the chain-ordered, rotationally isotropic phase discussed in the text.

namic stability dictates that the above curve must be concave at all temperatures. If there are coexisting phases then the curve will have a region in which the required concavity does not hold. A double tangent construction (27), illustrated in Fig. 5, then yields the concentrations of the coexisting phases.

The theoretical modeling procedure is applied to DPPC rather than DMPC (which was the model system for the simulations) because DPPC is the system examined experimentally by Vist and Davis (13).

IV. MODEL PHASE DIAGRAM

The phase diagram calculated for the model by the above procedure for the DPPC-cholesterol system is shown in Fig. 6. The lines on this diagram are boundaries along which two phases coexist. The three phases observed in the solutions to the minimization equations are: L_α, an isotropic fluid phase with nonnegligible fractions of the molecules in all accessible states; $L_{\beta'}$, an anisotropic phase in which only the smallest length rod state with a *single* orientation is populated; and a β phase. The β phase is characterized fully ordered chains, in which the shadow states corresponding to lipids with *gauche* chain conformations are unoccupied. However the system remains rotationally isotropic, so that all rotational states are equally populated.

The interplay among phases in this model is best pictured in the Free Energy vs. cholesterol concentration plot of Fig. 5. As the figure shows at the plotted temperature, T = 40.0°C, there are two double tangent constructions. One double tangent line connects an L_α phase at x_c = 3.5% to an $L_{\beta'}$ phase at x_c = 1.1%, and one connects an L_α phase at x_c = 5.0% to a β phase at x_c = 40.0%. Because the two tangent lines are distinct, there are two distinct regions of two phase coexistence. As the temperature is lowered, the L_α phase curve shifts upward until, at 39.5°C the two dotted double tangent lines coincide. This yields three coexisting phases, a $L_{\beta'}$ phase at 1% cholesterol, an L_α phase at 5% cholesterol, and a β phase at 40% cholesterol. Only at T = 39.5°C are there more than two coexisting phases.

As the enlarged area of Fig. 5 shows, there is also a point at ~0.5% at which the Free Energy curves for the $L_{\beta'}$ and the β phases cross. In this region differences in Free Energy between the $L_{\beta'}$ and the β phases become very small. Although the Free Energy curves for these two phases cross in Fig. 5 the difference is sufficiently small that the stable phase is still $L_{\beta'}$. That is, in the temperature range over which the crossing occurs, 41.4°C ≥ T ≥ 38°C, within the accuracy of the numerical method, the double tangent line contacts either the Free Energy curve for the pure $L_{\beta'}$ phase or the point where the $L_{\beta'}$ and β phase Free energy curves cross.

At temperatures below 38°C a single double tangent line runs from a $L_{\beta'}$ phase at $x_c \leq 0.5\%$ to a β phase at $x_c \geq 40\%$. This is the solid phase immiscibility region in the model. Although a stable $L_{\beta'}$ phase may be present for very small x_c, the phases are for practical purposes immiscible. Above the lipid chain melting temperature of 41.4°C the model system enters a coexistence region between fluid and β phases as soon as the cholesterol concentration rises above ~5%, and a pure β phase occurs at all temperatures at cholesterol content to the right of the coexistence line between ~40–60%.

At the qualitative level the calculated phase diagram compares well with the experimental diagram of Vist

and Davis (13) (after allowance for the different temperatures in the measurements due to the use of deuterated PC). Both experiment and theory show qualitatively similar types of phase sequences. The major quantitative differences between theory and experiment are: (*a*) the presence of the immiscibility region at low temperatures and (*b*) the location of the coexistence lines on the right-hand side of the diagram between the pure β phase and the two phase region are in the range of 40–60% cholesterol concentration in the theory, but are located between 20–30% in the experimental data. In the next section the above results are discussed.

V. DISCUSSION

The theoretical model described above was constructed from an earlier model for lipid phase transitions (19, 21) with qualitative input from the results of the MC simulation results described in Section II. The hard rod model provides a natural way to include the lipid-cholesterol interactions observed in the MC runs into a theoretical model which accurately includes the all-important hard core intermolecular packing interactions in its framework. To clearly identify the role of these interactions the model is kept as simple as possible. Therefore in the model the role of the cholesterol is simply to reduce the attractive van der Waals energy of the system slightly, and, more importantly, to reduce the statistical weights of the chain states. Then comparison of the model predictions with experiment reveals not only the limitations of the model, but may provide insight into the experimental data as well. As Fig. 6 shows the model predicts phase sequences which are in partial accord with the experimental phase diagram of Vist and Davis (13).

The critical properties of the model which are directly responsible for the predicted phases are firstly, the weight reduction factors, and, secondly, the dimension of the cholesterol molecule (both given in Table 1). The weight reduction factors are a natural way to express the effect of cholesterol on the lipid chain isomerization. Although the MC simulations sample lipid chain configuration space sufficiently to obtain accurate order parameter profiles and average number of gauche bonds per chain the number of different cholesterol-lipid microenvironments simulated is effectively only two (isolated cholesterols and pairs of cholesterols). This is insufficient to allow for extraction of a quantitative functional form for the weight reduction factors used in the theory. The weight reduction functions used in this work therefore represent the qualitative effect of isolated cholesterol molecules (the linear term in x_c), and pairs of cholesterol molecules (the quadratic term in x_c), on the chain states as observed in the simulations. The coefficients of the linear and the quadratic terms cannot, as explained above, be directly extracted from the simulations. Different weight reduction functions yield phase diagrams with the same qualitative features as Fig. 6, but with the phase boundaries at different cholesterol concentrations. The narrow region of $L_\alpha - L_{\beta'}$ coexistence is more senstitive to the nature of the weight reduction functions.

Above the chain melting temperature the theory and experiment are in full accord at lower cholesterol concentrations. At higher x_c the theory fails to predict the pure β coexistence line at ~25% cholesterol, instead placing this line between 40% and 60% cholesterol. Within about a degree below the chain melting transition, the model predicts a narrow two phase region consisting of L_α and $L_{\beta'}$ phases. The experimental phase diagram also contains a two phase region with a different shape at about the same location, in which L_α and $L_{\beta'}$ phases are identified as coexistent.

The appearance of the solid phase immiscibility in the model at low temperatures, and the marginal stability of the narrow region of $L_{\beta'}$ phase at low x_c are both consequences of the severe nature of the lipid-cholesterol packing mismatch due to the different molecular sizes. It is possible that the present model exaggerates this effect by using impenetrable hard rods and only a limited number of rotational states. However, it is also conceivable that the absence of a pretransition in the model brings the immiscible region closer in temperature to the main phase transition region. Although there is no indication of an immiscible solid phase region in the phase diagram of Vist and Davis (13), such a region has been proposed earlier based on spin label studies (9, 10). It is plausible that at *some* very low temperature such a region should exist in the experimental systems. The coexistence line at the high cholesterol side of the phase diagram is substantially higher than that observed by Vist and Davis (13). This suggests that at higher cholesterol concentrations, restrictions on lipid chains become even stronger than Table 1 allows.

It is important to point out that all of the model calculations are extremely sensitive to the dimensions and relative shapes of the constituent molecules. Calculations carried out with the cholesterol rod dimensions set at 6.8 Å (cap diameter) by 1.1 Å (rod length) show a different phase diagram, in which there is a homogeneous gel phase at very low cholesterol concentration, but there is no fluid-gel coexistence region in this case. It should be emphasized that the extremely rigid shapes and the shadow projection hypothesis which form the basis for this model are most suspect in solid phases.

The use of a two-dimensional hard rod model for lipid and cholesterol molecules in a bilayer is not without

drawbacks. Firstly, as mentioned in the previous section, the areas assigned to the hard rods are larger than minimal areas as measured from CPK models. This is required in the model to achieve the proper average area per molecule for the system. The intermolecular potential in the model contains only an attractive contribution, so that without the enlarged "effective" molecular state areas the model system would collapse to an unrealistically high density. The areas of the states used in the model, and given in Table 1, represent the area each molecule effectively excludes from all other molecules. Secondly, the mapping of many lipid chain states onto a few weighted rod states makes direct input from the simulations far more difficult. Thirdly, the low temperature orientationally ordered phase (Fig. 4, *top state*) literally represents a system in which all molecules have the planes of their hydrocarbon chains parallel. There is no evidence to suggest that this extreme orientation actually occurs (however in the gel phase in real bilayers there are likely to be domains within which there is locally parallel molecular orientation). It is clear that in the lipid gel ($L_{\beta'}$) phase there is little or no long axis molecular rotation due to the low area per molecule and to the anisotropic molecular shapes of the lipids. The orientationally ordered low temperature lipid phase of the theoretical model should be considered as an extreme caricature of a chain ordered phase in which molecular long axis rotation is forbidden. The mechanism which drives a transition from orientationally restricted states due to hard core packing to a state with unrestricted orientation freedom is *the same* in both cases, and is unambiguously described by this theoretical model.

The model presented in this paper has much in common with that of Ipsen et al. (14). Both models include degrees of freedom which are not related to with chain isomerization, and in both models these degrees of freedom are the relevant order–disorder variables for the formation of the β phase. The advantage of the model described in the present paper is that these degrees of freedom are explicitly assigned to molecular rotation states whereas in the model of Ipsen et al. the degrees of freedom are unspecified Potts-like spins associated with the lattice points. The β phase in our model is unambiguously associated with molecular rotational isotropy and ordered chains, and is a basic phase which occurs in general lipid crystalline systems consisting of hard objects of anisotropic shape (28).

We thank Dr. W. S. McCullough for a critical reading of the manuscript.

This work is supported in part by National Science Foundation grant DMB8703644 and utilized the Cray XMP/48 system at the National Center for Supercomputing Applications at the University of Illinois at Urbana-Champaign.

Received for publication 31 May 1900 and in final form 24 September 1990.

REFERENCES

1. Presti, F. T. 1985. The role of cholesterol in membrane fluidity. *In* Membrane Fluidity in Biology. Cellular Aspects. R. C. Aloia and J. M. Boggs, editors. Academic Press, NY. 4:97–146.
2. Mabrey, S., and J. M. Sturtevant. 1976. Investigation of phase transitions of lipids and lipid mixtures by high sensitivity differential scanning calorimetry. *Proc. Natl. Acad. Sci. USA.* 73:3862–3866.
3. Estep, T. N., D. B. Mountcastle, R. B. Biltonen, and T. E. Thompson. 1978. Studies on the anomalous thermotropic behavior of aqueous dispersions of dipalmitoylphosphatidylcholine-cholesterol mixtures. *Biochemistry.* 17:1984–1989.
4. Demel, R. A., K. R. Bruckdorfer, and L. L. M. van Deenen. 1972. Structural requirements of sterols for the interaction with lecithin at the Air-Water interface. *Biochim. Biophys. Acta.* 255:311–320.
5. Jacobs, R., and E. Oldfield. 1979. Deuterium nuclear magnetic resonance investigation of dimyristoyllecithin- and dipalmitoyllecithin-cholesterol mixtures. *Biochemistry.* 18:3280–3285.
6. Delmelle, M., K. W. Butler, and I. C. P. Smith. 1980. Saturation transfer electron spin resonance spectroscopy as a probe of anisotropic motion in model membrane systems. *Biochemistry.* 19:698–704.
7. Peng, Z. Y., N. Tjandra, V. Simplaceanu, and C. Ho. 1989. Slow motions in oriented phospholipid bilayers and effects of cholesterol or gramicidin. *Biophys. J.* 56:877–885.
8. Cornell, B. A., and M. Keniry. 1983. The effect of cholesterol and gramicidin A on the carbonyl groups of dimyristoylphosphatidylcholine dispersions. *Biochim. Biophys. Acta.* 732:705–710.
9. Shimshick, E. J., and H. M. McConnell. Lateral phase separations in binary mixtures of cholesterol and phospholipids. *Biochem. Biophys. Res. Commun.* 53:446–451.
10. Recktenwald, D. J., and H. M. McConnell. 1981. Phase equilibria in binary mixtures of phosphatidylcholine and cholesterol. *Biochemistry.* 20:4505–4510.
11. Lentz, B. R., D. A. Barrow, and M. Hoechli. 1980. Cholesterol-phosphatidylcholine interactions in multilamellar vesicles. *Biochemistry.* 19:1943–1954.
12. Mortensen, K., W. Pfeiffer, E. Sackmann, and W. Knoll. 1988. Structural properties of a phosphatidylcholine-cholesterol system as studied by small angle neutron scattering: ripple structure and phase diagram. *Biochim. Biophys. Acta.* 945:221–245.
13. Vist, M. R., and J. H. Davis. 1990. Phase equilibria of cholesterol/dipalmitoylphosphatidylcholine mixtures: ^{2}H nuclear magnetic resonance and differential scanning calorimetry. *Biochemistry.* 29:451–464.
14. Ipsen, J. H., G. Karlström, O. G. Mouritsen, H. Wennerstrom, and M. J. Zuckermann. 1987. Phase equilibria in the phosphatidylcholine-cholesterol system. *Biochim. Biophys. Acta.* 905:162–172.

15. Scott, H. L., and S. Kalaskar. 1989. Lipid chains and cholesterol in model membranes: a Monte Carlo study. *Biochemistry.* 28:3687–3692.

16. Scott, H. L. 1990. Computer aided methods for the study of lipid chain packing in model membranes and micelles. *In* Molecular Description of Biological Membrane Components by Computer Aided Conformational Analysis. R. Brasseur, editor. CRC Press, Boca Raton, FL. 49 pp. In press.

17. Seelig, J., and P. M. Macdonald. 1987. Phospholipids and proteins in biological membranes. ^{2}H NMR as a method to study structure, dynamics, and interactions. *Accounts of Chemical Research.* 20:221–228.

18. Nagle, J. F. 1980. Theory of the main lipid bilayer phase transition. *Annu. Rev. Phys. Chem.* 31:157–192.

19. Scott, H. L. 1981. Lecithin bilayers: a model which describes the main and lower phase transitions. *Biochim. Biophys. Acta.* 643:161–167.

20. Scott, H. L., and W. H. Cheng. 1979. A theoretical model for lipid mixtures, phase transitions and phase diagrams. *Biophys. J.* 28:117–132.

21. Scott, H. L. 1982. Phase transitions in lipid bilayers: a theoretical model for phosphatidylethanolamine and phosphatidic acid bilayers. *Biochim. Biophys. Acta.* 648:129–136.

22. Reiss, H., J. L. Lebowitz, and H. L. Frisch. 1959. Statistical mechanics of rigid spheres. *J. Chem. Phys.* 31:369–380.

23. Scott, H. L., and P. A. Pearce. 1989. Calculation of intermolecular interaction strengths in the $P_{\beta'}$ phase in lipid bilayers. *Biophys. J.* 55:339–345.

24. McCullough, W. S., and H. L. Scott. 1990. Statistical mechanical theory of the ripple phase of lipid bilayers. *Phys. Rev. Lett.* 65:931–934.

25. Goltstein, R., and S. Leibler. 1988. Model for lamellar phases of interacting lipid membranes. *Phys. Rev. Lett.* 61:2213–2215.

26. Rothmann, J. E., and D. M. Engleman. 1972. Molecular mechanism for the interaction of phospholipid with cholesterol. *Nature New Biol.* 237:42–44.

27. Callen, H. B. 1985. Thermodynamics and an Introduction to Thermostatistics. Wiley, New York. 243–252.

28. de Gennes, P. G. 1974. The Physics of Liquid Crystals. Clarendon Press, Oxford. 46–48.